

Equilibrium Aspects of Folded Chain Polymer Crystals

Buckley Crist

Department of Materials Science and Engineering and Department of Chemical and Biological Engineering, Northwestern University, Evanston, Illinois 60208

Received September 19, 2005; Revised Manuscript Received December 8, 2005

ABSTRACT: Recent simulations of polymer crystallization have stimulated questions about thermodynamic vs kinetic control of thickness in folded chain crystals. Free energy landscapes and equilibrium crystal thickness L^* and width W^* are analyzed for a polyethylene-like material with classical nucleation and growth and with a similar polymer theory that includes entropy effects from folds and cilia. Small crystals that form from one or a few macromolecules must contain folded chains; these equilibrium structures grow with constant aspect ratio $L^*/W^* = \sigma_e/\sigma_s$, the quotient of basal and lateral specific surface energies. The fold/cilium entropy increases the effective σ_e , leading to crystals that are about 50% thicker than the classical L^* . Another consequence of the surface entropy is an equilibrium amorphous fraction that increases with crystallization temperature T_c . Equilibrium crystal growth requires that thickness L^* increase by refolding previously crystallized stems until the extended chain thickness L_{\max} is achieved, at which point folding is no longer energetically favored. Equilibrium folded chain crystals are expected when system size is small and when rearrangements are feasible. Crystallization of isolated chains from very dilute solution, by experiment or by dynamic simulation, indeed gives what appear to be equilibrium folded chain crystals. Simulations also reveal a global collapse mechanism that does not conform to nucleation and growth.

Introduction

The first postulate that polymer crystals have folded chain habits was made in 1938 by Storks after analyzing the electron diffraction pattern of a thin film of *trans*-polyisoprene.¹ This prescient notion was confirmed 19 years later by Keller's electron microscopy and diffraction studies of ca. 10–15 nm thick lamellar polyethylene crystals grown from dilute solution.² Important observations are that crystal thickness L is insensitive to molecular weight and that it increases with crystallization temperature T_c .

Explanations, classified as kinetic or equilibrium in nature, were soon put forth to account for temperature-dependent chain folding in polymer crystals. Lauritzen and Hoffman³ pioneered the kinetic approach with secondary nucleation from dilute solution leading to folded chain crystals with thickness L that is just sufficient to prevent melting at the crystallization temperature T_c . Primary nuclei were assumed to be chain folded as well, a topic considered later in this paper. The LH model was soon extended to crystallization from the melt;⁴ a comprehensive review of LH theory and alternative approaches to secondary nucleation in polymer crystal growth (not primary nucleation) has been presented by Armistead and Goldbeck-Wood.⁵ Returning to equilibrium theories for folding, two were proposed in the 1960s. Peterlin and Fischer⁶ considered the effect of thermally activated chain vibrations on the crystal free energy, which is minimized at a particular temperature-dependent L . Peterson and Lindenmeyer treated dangling chain ends (cilia) that create an entropic energy penalty unless the fold period and chain length are such that the chain ends are at the basal surfaces.⁷ Local energy minima occur when the cilia lengths are zero and the number of folds per chain is 4 or 3 or 2, etc.; the energy is lowest for zero folds (extended chain crystals) for monodisperse chains. However, additional entropy terms for a mixture of different length chains lead to a single minimum free energy of crystallization at an average lamellar thickness L that increases with crystallization temperature.

The Peterson–Lindenmeyer model is of interest because it utilizes the conformational entropy of noncrystalline portions of the chain in evaluating the free energy of the “crystal”. Recall that chain portions generally exist in both crystalline and noncrystalline regions, so a complete description of the free energy requires both states, a concept with a long but sparse history that dates from 1949.⁸ Flory calculated the entropic effects of excluding chain ends from fringed micelle (not chain folded) crystals, but he ignored conformations of the noncrystalline tails. For chains of degree of polymerization x , equilibrium is characterized by crystalline stems with $m < x$ units and crystalline fraction $\varphi_c = m/x < 1$ that both approach zero at the final melting temperature $T_m(x)$, the latter being less than T_m^0 for infinitely long chains (no ends). Flory considered equilibrium crystallization, which is the reverse of melting. In his scenario the equilibrium crystal thickness *decreases* as the crystallization temperature is raised toward $T_m(x)$. Mandelkern et al. used Flory's entropy-modified free energy to calculate primary critical nucleus dimensions and barrier heights for fringed micellar crystals.⁹ They also noted that the molecular weight dependent $T_m(x)$ is the proper reference for defining undercooling and nucleation barriers. Zachmann^{10,11} and others^{12,13} extended entropy calculations to the conformations of folds and cilia on the basal surfaces of polymer crystals, an approach that leads to reversible “surface melting” of chain folded lamellae.^{14,15} Ishinabe¹⁶ revisited the Peterson–Lindenmeyer problem and included the entropic effect of adjacent reentry folds of variable length. The result for monodisperse chains is qualitatively the same as that for ref 7, with the additional idea that thickening to the equilibrium extended chain state is prevented by large energy barriers. Chen et al.¹⁷ embellished Ishinabe's approach with a lateral surface energy and predicted the equilibrium shape for the folded chain crystal formed by a single polymer molecule.

The chain-end and fold/loop entropies described above have been neglected in virtually all treatments of polymer crystal thermodynamics since the discovery of folded chain habits

* Corresponding author. E-mail: b-crist@northwestern.edu.

nearly 50 years ago. An exception is the use of the Flory–Vrij equation¹⁸ to correct the equilibrium melting point T_m^0 for finite degree of polymerization x , even though that approach is strictly valid only for extended chain crystals with uniform degree of polymerization x . Over the same time period there has been near unanimous agreement that chain folding during crystal growth derives from kinetic factors that establish metastable lamellar habits; achievement of equilibrium extended chain crystals is prevented by secondary nucleation barriers that are fundamentally enthalpic in nature, although the lateral surface energy density can be rationalized by entropic arguments.¹⁹ With very few exceptions, analyses of growth rates of folded chain crystals have been with the analytically tractable LH theory.^{3–5}

A recent complement to theory and experiment is simulation. Molecular dynamics studies of polymer crystallization from dilute solution (low chain density), pioneered by Kavassalis and Sundararajan,²⁰ are of particular interest because homogeneous primary nucleation and subsequent growth of folded chain crystals are unambiguous. Such studies can provide detailed information on the phase transformation, but it must be kept in mind that the system size is small, typically about 10^3 united atoms or “beads” corresponding to single polyethylene chain with a molecular weight of 14 kg/mol. It is self-evident that a single extended chain is unstable at all temperatures, while for $T < T_m$ a single chain will adopt an ordered state that must include folds of some sort. Is the thickness L of this small crystal dictated by kinetic or equilibrium factors? How is crystal size affected by the number of chains in the system? Do simulations with small systems have experimental counterparts? These are the questions addressed in this paper.

Of particular interest is the analysis of Langevin dynamics simulations of polymer crystallization from dilute solution by Muthukumar.²¹ The relative populations of crystals of different thickness were used to infer that the fold period is established by free energy, not by kinetic barriers. An analytical model was proposed that predicts a free energy minimum for folded chain crystals with thickness L less than the fully extended chain length L_{\max} . That model, which is more comprehensive than other treatments that include entropy, is the basis for the present consideration of thermodynamically controlled sizes in polymer crystallization. It is shown that dimensions established by equilibrium conditions are important during homogeneous primary nucleation and in the early stages of the growth of supercritical nuclei.

Classical nucleation and growth are considered first. This approach, while not including polymer characteristics, nevertheless establishes the basis for equilibrium crystal dimensions. Then a variation of Muthukumar’s model is employed to assess primary nucleation and growth of polymer chains from dilute solution. Crystal dimensions are established for folded chain structures, and the equilibrium thickness $L^* \sim V^{1/3}$ increases with the cube root of the crystal volume V . A perhaps unexpected corollary is the existence of an equilibrium non-crystalline fraction for polymer crystals.

Classical Nucleation and Growth

The polymer crystal is assumed to have transverse isotropy, its shape represented by a square tablet or column of width W and thickness L as in Figure 1. The free energy of this crystal with respect to the disordered melt or solution state is

$$\Delta G = -W^2 L \Delta G_v + 4WL\sigma_s + 2W^2\sigma_e \quad (1)$$

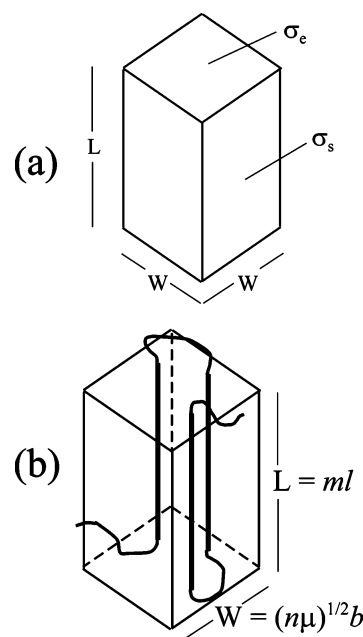


Figure 1. Representations of a transversely isotropic crystal: (a) illustrates dimensions and surface energies; (b) illustrates a single chain with $\mu = 3$ stems in the crystal, $\mu - 1 = 2$ folds, and 2 cilia.

Here $\Delta G_v = \Delta H_v(T_m^0 - T)/T_m^0$ is the bulk free energy of melting (or dissolution) per unit volume (J/m^3) where ΔH_v is the enthalpy and T_m^0 is the melting (or dissolution) temperature of a perfect crystal. Specific surface energies σ_s and σ_e (J/m^2) are for the lateral (side) and basal (end) surfaces, respectively.

Classical nucleation theory leads to the critical dimensions for the *smallest* homogeneous nucleus that becomes more stable for growth in any direction—both thickness and width will increase spontaneously. Partial differentiation of ΔG with respect to L and W gives the coordinates of the saddle point on the free energy surface:

$$\begin{aligned} L_c &= \frac{4\sigma_e}{\Delta G_v} \\ W_c &= \frac{4\sigma_s}{\Delta G_v} \end{aligned} \quad (2)$$

Contours of the free energy surface $\Delta G(L, W)$ are presented in Figure 2 for polyethylene crystallizing at an undercooling $\Delta T = T - T_m^0 = 50$ K, in the midrange of experimental values associated with homogeneous nucleation.¹¹ With energy expressed in units of kT , the parameters are²² $G_v = 6.6/\text{nm}^3$ ($\Delta H_v = 285 \text{ mJ/m}^3$, $T_m^0 = 419 \text{ K}$), $\sigma_e = 17.7/\text{nm}^2$ (90 mJ/m^2), and $\sigma_s = 2.3/\text{nm}^2$ (11.8 mJ/m^3). Most conspicuous is the saddle point marked by \oplus , where the energy is $\Delta G_c = 32\sigma_s^2\sigma_e/\Delta G_v^2 = 69kT$. The dashed arrow indicates only that the energy path to the critical point is an uphill one; the critical nucleus is formed by one or more thermally driven fluctuations that supply the energy required to assemble the small structure. Critical dimensions from eq 2 are $L_c = 10.8 \text{ nm}$ and $W_c = 1.4 \text{ nm}$, and the critical volume is $V_c = 21.2 \text{ nm}^3$, corresponding to ca. 440 C_2H_4 units or a polyethylene chain with a molecular weight $M \approx 12 \text{ kg/mol}$. The geometry of this critical nucleus calls for 10–11 crystalline stems (stem cross section is 0.19 nm^2), each composed of about 43 C_2H_4 groups (monomer length $l = 0.254 \text{ nm}$).

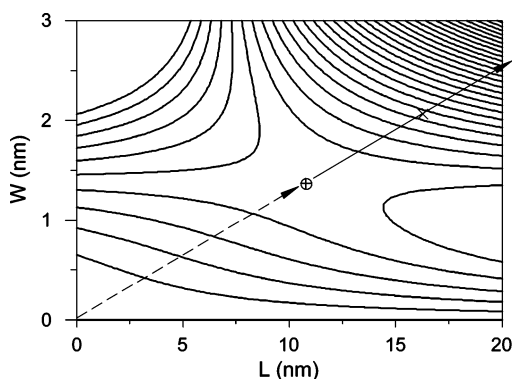


Figure 2. Contour plot of the classical free energy surface eq 1 with values in the text. The saddle point for critical dimensions $W_c = 1.41$ nm and $L_c = 10.8$ nm is indicated by \oplus and the stability point with $L_{st} = 16.2$ nm and $W_{st} = 2.12$ nm by \times . Dashed and solid arrows indicate uphill and downhill energy paths, respectively. The solid arrow is for growth at the aspect ratio $L/W = \sigma_e/\sigma_s$ that minimizes the free energy density of the crystal; see text.

How do dimensions evolve as the crystal grows at constant temperature beyond the size of the critical nucleus? The equilibrium dimensions for a crystal are obtained by minimizing the free energy in eq 1, subject to the volume $V = W^2L$ having a particular value:

$$\begin{aligned} L^* &= \left(\frac{\sigma_e}{\sigma_s}\right)^{2/3} V^{1/3} \\ W^* &= \left(\frac{\sigma_s}{\sigma_e}\right)^{1/3} V^{1/3} \end{aligned} \quad (3)$$

Crystal volume V and equilibrium dimensions L^* and W^* increase in tandem by accretion of monomers from either the nucleating chain or from other chains. Growth at the equilibrium shape is indicated by the solid arrow (downhill energy) in Figure 2. The minimum-energy aspect ratio is independent of crystal size and is the same for both the critical nucleus (from eq 2) and a stable crystal of arbitrary volume (from eq 3):

$$\frac{L^*}{W^*} = \frac{L_c}{W_c} = \frac{\sigma_e}{\sigma_s} \quad (4)$$

Equation 4 can be recognized as an example of Wulff's law^{23,24} for equilibrium crystal shapes. It should be noted that the same surface energies are used for critical nuclei and for mature crystals, a common simplifying assumption that may not be correct in all cases.

Although the free energy of the supercritical nucleus decreases during growth, it remains higher than that of the melt until the stability dimensions L_{st} and W_{st} are achieved for which $\Delta G = 0$ in eq 1:

$$\begin{aligned} L_{st} &= \frac{6\sigma_e}{\Delta G_v} \\ W_{st} &= \frac{6\sigma_s}{\Delta G_v} \end{aligned} \quad (5)$$

The nucleus must grow until linear dimensions exceed 1.5 times the critical ones before the small crystal is the energetically preferred state, which is indicated in Figure 2 by the symbol \times .

The same thermodynamic condition ($\Delta G = 0$) can be used to establish the melting temperature T_m of an equilibrium crystal of volume $V = W^2L^*$:

$$\begin{aligned} T_m &= T_m^0 \left(1 - \frac{6\sigma_e^{1/3}\sigma_s^{2/3}}{\Delta H_v V^{1/3}}\right) \\ &= T_m^0 \left(1 - \frac{6\sigma_e}{\Delta H_v L^*}\right) \\ &= T_m^0 \left(1 - \frac{6\sigma_s}{\Delta H_v W^*}\right) \end{aligned} \quad (6)$$

Equation 6 is the Gibbs–Thomson equation for small crystals destabilized by surface energies. The size of the equilibrium crystal is expressed equivalently in terms of volume, thickness, or width. When a growing nucleus achieves the stable dimensions L_{st} and W_{st} , the melting temperature T_m is equal to the crystallization temperature T_c . With subsequent growth, T_m increases above T_c , and the crystal becomes thermodynamically stable with respect to the melt. Hu et al.²⁵ have considered some aspects of crystallizing and melting small polymer systems using expressions like the classical eq 1 that lack (entropic) effects of partially noncrystalline chains.

Some discussion of the three sets of dimensions (critical, stability, and equilibrium), each having the same aspect ratio σ_e/σ_s , is appropriate. The general definition of an equilibrium point is one for which all free energy gradients are zero;²⁶ of the variables W , L , V , and aspect ratio L/V used here, only two are independent, and the usual choices are W and L . Hence, the critical point defined by eq 2 is an unstable equilibrium point (saddle point). An important concept for this paper is that the critical dimensions L_c and W_c are established by thermodynamic, not kinetic, criteria. The equilibrium dimensions L^* and W^* (eq 3) are somewhat different in character because the free energy ΔG (eq 1) is unbounded in an open system. Only for a prescribed crystal volume V can one define an equilibrium condition (free energy gradients of zero magnitude); the dimensions L^* and W^* define a stable equilibrium point corresponding to the minimum free energy density of the crystal. Finally, the stability point L_{st} , W_{st} is that for which the free energy of the small crystal is the same as that of the melt. This state is defined by the equality of ΔG at two points on the energy surface, not by energy gradients at a single point. As each of these three states is characterized by the same aspect ratio $L/W = \sigma_e/\sigma_s$, the solid arrow in Figure 2 is the path of minimum free energy density $\Delta G/V$ of the crystal.

While no reference has been made to the chainlike nature of polymer molecules in the derivations of eqs 1–6, one can add polymer features after the fact. Consider first a single polyethylene chain with a molar mass $M = 120$ kg/mol ($x = 4286$). Homogeneous nucleation at $\Delta T = 50$ K, described above, gives a critical nucleus that comprises only 10% of the chain. Recall that this critical nucleus contains 10–11 stems; one possible state has 9–10 hairpin folds, but other intramolecular arrangements are possible. Subsequent isothermal growth can be envisioned by folding adjacent portions of the amorphous tails onto the existing crystal, but the fold period must increase to maintain the equilibrium dimensions dictated by eq 3. Stability is achieved (eq 5) when $L_{st} = 16.1$ nm and $W_{st} = 2.1$ nm, corresponding to 34% of the chain being crystallized. As only one polymer molecule is present, the entire chain subsequently becomes incorporated into the final crystal having 10 times the critical volume, thickness $L_1^* = 10^{1/3}L_c = 23.3$ nm (92

monomers per stem), and $W_1^* = 10^{1/3}W_c = 3.0$ nm (47 stems); the subscript "1" is for a one-chain crystal.

Provided that the system is closed—comprised in this instance of a single polymer molecule—an equilibrium folded chain crystalline state has been achieved with 46 folds that are implicitly crystallographic because the entire chain is crystalline. However, this state is unstable in the presence of additional polymer that can crystallize and further lower the free energy. Consider for example a set of 50 chains of $M = 120$ kg/mol at the same undercooling. Dimensions L_c and W_c of the critical nucleus are unchanged, but that structure could be composed of stems from 10 to 11 *different* chains in a fringed micelle. For 50 chains the final equilibrium sizes are $L^* = (50 \times 10)^{1/3}L_c = 85.7$ nm (337 monomers per stem) and $W^* = 7.94W_c = 11.1$ nm (649 stems). This crystal contains 649 stems deriving from 12 folds per chain; note that the number of folds per chain drops as the crystal grows (L^* increases). Folding for a completely crystallized system is required geometrically whenever the number of stems (proportional to W^{*2}) exceeds the number of chains n . The equilibrium condition obviously changes when n is increased to the point where L^* equals the maximum thickness $L_{\max} = 1089$ nm for this particular polyethylene with $M = 120$ kg/mol. One can show that the crossover to extended chain crystallization occurs when the number of chains is $n_{ec} = (W_1^{*2}/0.19 \text{ nm}^2/\text{stem})^3$ or $n_{ec} = 104\,000$ in the present example (depending in general on x^2 and independent of ΔT). For $n \geq n_{ec}$, the equilibrium thickness is $L^* = L_{\max}$, corresponding to the conventional equilibrium state with no folds. Within the extended chain regime the crystal width is defined by $W^2 = V/L_{\max}$. Other possibilities can be envisioned: If the fold period is unable for kinetic reasons to increase according to eq 3, lateral crystal growth at constant $L' \geq L_c$ is energetically favored for $W' \geq W_c$. Here the larger, nonequilibrium width is defined by $W'^2 = V/L'$.

To summarize this section, classical homogeneous nucleation gives rise to a critical nucleus with thickness L_c and width W_c that are inversely proportional to undercooling ΔT . This unstable structure is predicted to grow at constant aspect ratio $L^*/W^* = L_c/W_c = \sigma_e/\sigma_s$; for a system with a restricted amount of material the final equilibrium dimensions are prescribed by eq 3. Chain folding is necessary for homogeneous nucleation and crystal growth of a single chain or a few chains (very dilute solution, simulations). Regardless of the number of chains, equilibrium chain folding is similarly favored when $L^* < L_{\max}$ or, equivalently, $n < n_{ec}$. Critical nucleus dimensions L_c and W_c are independent of chain length and the number of chains, but the equilibrium crystal sizes L^* and W^* are proportional to $x^{1/3}$ and to $n^{1/3}$ (eq 3). Equilibrium crystallization will convert to the extended chain habit for systems with a very large number of chains in excess of n_{ec} . Should the crystal for any reason be unable achieve the equilibrium thickness L^* , lateral growth of width W' at smaller thickness $L^* > L' \geq L_c$ is permitted energetically.

Polymer Crystallization and Growth

The free energy of crystallization in eq 1 can be modified to include the polymeric nature of the crystallizing material by considering explicitly the disordered parts of each of the n chains associated with the crystal as sketched in Figure 1b. Each chain has x monomers and contributes μ stems of m monomers to the crystal; μm is the number of crystalline repeats per chain, leaving $x - \mu m$ amorphous monomers that comprise $\mu - 1$ folds or loops and two cilia or tails. The crystal thickness is $L = ml$ and the crystal width is $W = (n\mu)^{1/2}b$, where l is the projected length

of a monomer and b is the separation between adjacent chain stems in the crystal.

Following Muthukumar,²¹ the free energy of the crystal is written as

$$\Delta G = -W^2L\Delta G_v + 4WL\sigma_s + 2W^2\sigma_e - nkT \ln Z \quad (7)$$

The first three terms are exactly those for classical nucleation and growth in eq 1. The fourth term derives from the entropy of n polymer molecules that participate in the crystal, each containing loops and tails that are situated on the basal fold surfaces. Z is proportional to the number of ways a single chain may appear in the crystal if it is composed of μ stems, $\mu - 1$ loops, and two tails; a greater Z (more folds, more shorter stems) will lower the free energy ΔG . There are two contributions to the number of chain states Z , the first based on the number of stems per chain μ , with the assumption that the direction of folds connecting the stems is unrestricted in the basal plane. (Perfectly regular folding yields only one distinguishable state, regardless of μ .) The second entropic contribution is from configurations of the folds which are treated as Gaussian loops. This part tends to increase the loop/tail length and the amorphous fraction φ_{am} . The reader is referred to the Appendix and to ref 21 for details on the formulation of Z , the following properties of which are adequate for the present discussion. For $\mu = 1$ (no folds), Z approaches 1 from above as m approaches x ; the maximum crystal thickness is bounded by $L_{\max} = xl$, a feature that is lacking in eq 1. Moreover, Z approaches zero when $\mu > 1$ (a fold is present) and m approaches x ; it is impossible to have complete crystallinity when the chain is folded. Hence, the entropic $\ln Z$ term in eq 7 diverges to infinity, creating a trough in the free energy surface for all combinations of $\mu m \approx x$. Note that folds and tails are noncrystalline in this treatment, while folds were implicitly crystalline and tails were ignored in the classical model described in the previous section. There is a minimum in ΔG at some combination of μ^* (corresponding to equilibrium area W^{*2}) and m^* (corresponding to equilibrium thickness L^*). The same condition defines the equilibrium noncrystalline fraction $\varphi_{\text{am}} = (x - \mu m^*)/x$.

The polymer aspects of the model are more apparent if W and L in eq 7 are expressed as $(n\mu)^{1/2}b$ and ml , respectively. Dividing the resulting expression by nkT , one obtains for the free energy of a chain Δg_{ch} :

$$\frac{\Delta g_{\text{ch}}}{kT} = -\mu mb^2l\Delta G_v + \frac{4}{n^{1/2}}\mu^{1/2}mb\sigma_s + 2\mu b^2\sigma_e - \ln Z \quad (8)$$

Here all energies on the right side are explicitly in units of kT . Equation 8 includes two features not found in Muthukumar;²¹ the second term on the right side has a factor of $n^{-1/2}$ to apportion correctly the lateral surface energy, and the third term has a conventional (enthalpic) basal specific surface energy σ_e that is not zero.

The effect of the entropic term $\ln Z$ on the free energy surface is illustrated with Figure 3a,b. Energy parameters are the same as those used in Figure 2 ($\Delta T = 50$ K); for this example, the degree of polymerization is $x = 1000$ and the number of chains is $n = 2$. Width W is represented by the metric $\mu^{1/2}$ and the thickness L by m , a convention used to distinguish polymer theory (eq 8) from classical theory (eq 1). Figure 3a represents the classical free energy surface calculated without the final entropic term in eq 8, and it corresponds exactly to Figure 2. The saddle point coordinates $\mu_c^{1/2} = 2.3$ (about 5 stems/chain) and $m_c = 42.8$ are easily derived from eq 2 with the aid of the projected monomer length $l = 0.254$ nm and the interstem

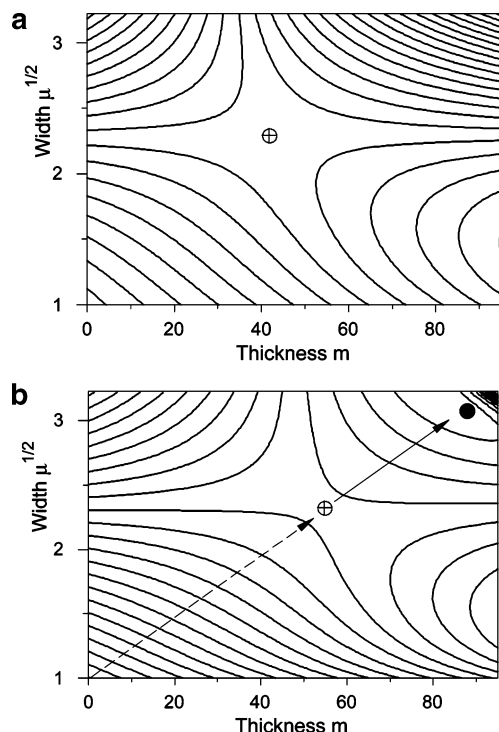


Figure 3. Contour plots of free energy surfaces for two chains of degree of polymerization 1000 ($n = 2$, $x = 1000$) in terms of width index $\mu^{1/2}$ and thickness index m ; undercooling and energies are the same as those in Figure 2. (a) is for the classical free energy expression, eq 8 without the final term; the saddle point indicated by \oplus corresponds exactly to that in Figure 2. (b) is for the complete free energy surface with the entropic term in eq 8; the saddle point is indicated by \oplus and the local (metastable) energy minimum by \bullet . The spacing of contour lines is the same in (a) and (b). As in Figure 2, arrows indicate uphill (dashed) and downhill (solid) paths.

separation $b = 0.44$ nm. Including the $\ln Z$ term has two effects. The energy surface represented in Figure 3b is sloped so the saddle point is shifted to larger thickness $m_c = 55$ with no discernible change in the critical width $\mu_c^{1/2} = 2.3$, and a local minimum in $\Delta g_{ch}/kT$ is seen at $\mu^{*1/2} = 3.1$ (ca. 10 stems per chain) and $m^* = 88$. The amorphous fraction is $\varphi_{am} = 0.14$ at the local minimum that in this case is metastable; the energy of the partially crystallized chain here always exceeds that of the amorphous polymer. This metastable case was chosen for illustration because the energy minimum is clearly displayed in the contour plot. Equation 8 does not lend itself to analytical derivatives, so coordinates of the saddle point and the minimum were established by numerical analyses of the free energy surface. As in Figure 2, the dashed arrow indicates only that the energy is uphill, and the solid arrow is for the downhill energy path that links the unstable saddle point and the free energy minimum. The aspect ratio $m^*/(n\mu^*)^{1/2}$ increases slightly along that line.

Undercooling. The number of chains is increased to $n = 4$ to provide adequate material for nucleation at smaller undercoolings. Maintaining $x = 1000$, the effects of undercooling $\Delta T = 33, 40, 50$, and 100 K on the critical dimensions represented by m_c and $\mu_c^{1/2}$ are summarized in Figure 4. Behaviors of the equilibrium dimension metrics m^* and $\mu^{*1/2}$ are quite different, as shown in Figure 5; hollow symbols indicate that the local energy minimum for $\Delta T = 33$ K is metastable. The picture that emerges is as follows: Homogeneous nucleation is achieved with a critical nucleus thickness m_c that is about 1/3 larger than the classical value (solid line in Figure 4), while the nucleus width $W_c \sim \mu_c^{1/2}$ conforms to the classical value (dashed line in Figure 4). Thickness m_c is

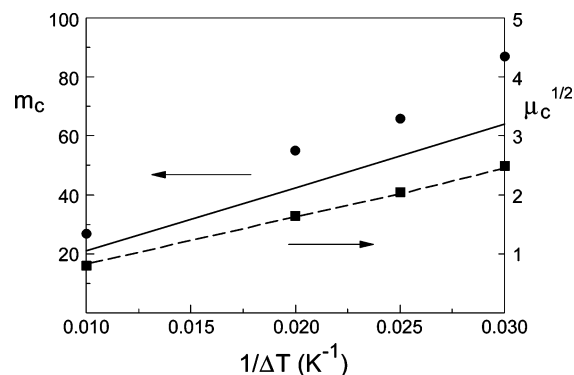


Figure 4. Dependence of critical nucleus size parameters m_c (\bullet) and $\mu_c^{1/2}$ (\blacksquare) on inverse undercooling ΔT^{-1} for $n = 4$ chains of degree of polymerization $x = 1000$. The lines are calculated for classical homogeneous nucleation parameters m_c (---) and $\mu_c^{1/2}$ (—).

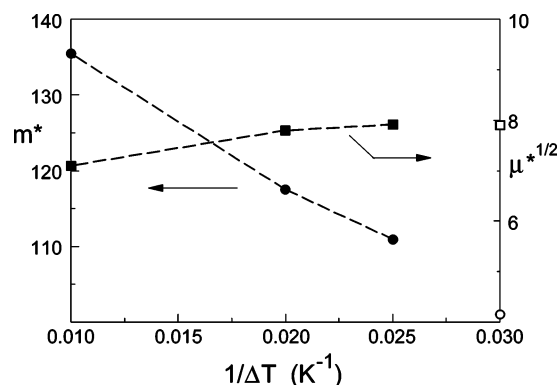


Figure 5. Dependence of equilibrium size parameters m^* (\bullet) and $\mu^{*1/2}$ (\blacksquare) on inverse undercooling ΔT^{-1} for $n = 4$ chains of degree of polymerization $x = 1000$. Lines are to guide the eye. Open data points for $\Delta T^{-1} = 0.03$ K⁻¹ indicate that the local free energy minimum is metastable at that temperature.

enlarged because the entropic term in eq 7 or eq 8 is a de facto basal surface energy that derives from loops and tails on the surface; hence, the effective “ σ_e ” in eq 2 is increased from the classical value. The critical thickness measure m_c grows more than linearly with ΔT^{-1} in Figure 4 because the entropic $\ln Z$ term is more significant at larger T_c (smaller ΔT). Lateral size $\mu_c^{1/2}$ is unaffected by the entropic term. Turning now to equilibrium dimensions in Figure 5, thickness m^* is seen to decrease with higher crystallization temperature (larger ΔT^{-1}), while the width measure $\mu^{*1/2}$ is essentially constant over the same range. The first of these equilibrium changes is qualitatively similar to the effects calculated by Flory⁸ and for surface melting of lamellae;¹⁵ the crystal becomes thinner, and the amorphous surface layer becomes thicker as the crystallization temperature is raised. However, the small increase in equilibrium width $\mu^{*1/2}$ with ΔT^{-1} is a reminder that the number of folds per chain is temperature dependent, so isothermal crystallization at different T_c is not directly comparable to surface melting. The change of amorphous fraction φ_{am} with undercooling (crystallization temperature) is shown in Figure 6. Note also that the equilibrium crystal aspect ratio represented by $m^*/(n\mu^*)^{1/2}$ decreases as T_c is raised, mainly from the decrease of m^* that derives from larger amorphous layer thickness.

It should be emphasized that the polymer model accounts only for equilibrium dimensions and the related noncrystalline fraction and loop surface thickness. No information is provided on fold or loop lengths, directions, distributions, etc. Furthermore, the fold surface is assumed to be normal to the crystalline chains.

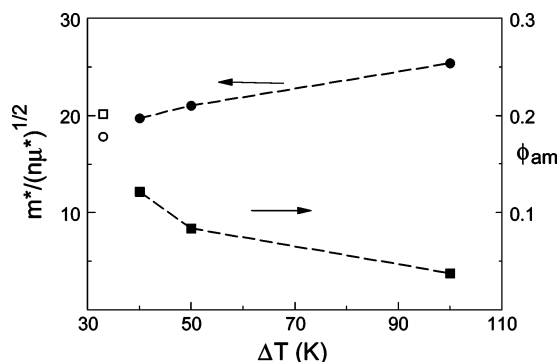


Figure 6. Crystal aspect ratio $m^*/(n\mu^*)^{1/2}$ (●) and amorphous fraction ϕ_{am} (■) for equilibrium established by $n = 4$ chains of degree of polymerization $x = 1000$ as a function of undercooling ΔT . Open data points for $\Delta T = 33$ K indicate that the local free energy minimum is metastable.

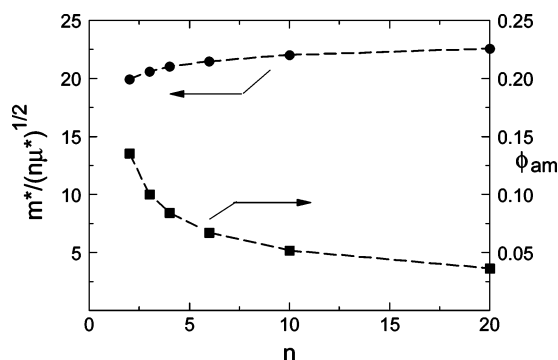


Figure 7. Crystal aspect ratio $m^*/(n\mu^*)^{1/2}$ (●) and amorphous fraction ϕ_{am} (■) for equilibrium established by different numbers of chains n of degree of polymerization $x = 1000$ at undercooling $\Delta T = 50$ K. Data points for $n = 2$ are for the metastable local equilibrium in Figure 3.

Number of Chains. The system size may be altered through the number of chains n . Just as with classical nucleation and growth, the free energy of a supercritical structure is lowered by the addition of more crystallizing polymer. Results are summarized in Figure 7 at an undercooling of 50 K for n between 2 and 20 with chains for which $x = 1000$; it was mentioned above that the local equilibrium for $n = 2$ is metastable. Equilibrium thickness m^* and width $(n\mu^*)^{1/2}$ both increase approximately as $n^{1/3}$ (see eq 3); hence, the aspect ratio $m^*/(n\mu^*)^{1/2}$ is nearly constant. For reference, the classical equilibrium aspect ratio is 13 in this format; inclusion of the entropic $\ln Z$ term in the free energy increases the equilibrium thickness of the crystal by $\sim 70\%$ (larger effective “ σ_e ”). Of equal interest is the equilibrium amorphous fraction ϕ_{am} , which decreases substantially from 0.136 to 0.036 over the range of n from 2 to 20 in Figure 7. The primary cause for this change is the growth of equilibrium stem length m^* with $n^{1/3}$, while the thickness of the amorphous layer (loops and tails) does not increase at constant T_c . In fact, the amorphous layer thickness decreases by about 40% for reasons that are not obvious, although the number of loops per chain is being reduced ($\mu^* \sim n^{-1/3}$) while two tails are maintained.

Plots vs $1/n$ (not shown) give asymptotic values at very large n of $\phi_{\text{am}} \rightarrow 0.01$ and $m^*/(n\mu^*)^{1/2} \rightarrow 23.5$ for equilibrium folded chain crystals. As with the classical theory, there is a crossover to extended chain equilibrium when $m^* \rightarrow x$ and $\mu^* \rightarrow 1$, giving rise to $n_{\text{ec}} = (1000/23.5)^2 = 1811$ in the present example. For this number of chains and above, the equilibrium crystal grows with thickness $L_{\text{max}} = 254$ nm. The amorphous fraction ϕ_{am} is invariant with n in the extended chain range, but it increases

with T_c in a manner reminiscent of Flory’s first treatment of surface melting.⁸

Degree of Polymerization. An alternative way to change the system size is by the degree of polymerization x while leaving the number of chains n fixed. Calculations (not shown) for $n = 2$ and $\Delta T = 50$ K give results very similar to those when increasing the number of chains; once again equilibrium thickness m^* and width $(n\mu^*)^{1/2}$ (in this case $\mu^{1/2}$) each scale approximately as $x^{1/3}$, and the aspect ratio $m^*/(n\mu^{1/2})$ drifts slowly upward to a limiting value of ca. 23.5 at very large x . Equilibrium noncrystalline fraction ϕ_{am} again decreases to a limit of about 0.01, but in this case the fraction of chain ends (tails) is decreasing. As stated in the preceding subsection, the reason for the decrease in amorphous layer thickness in larger (more crystalline) systems is not understood.

Discussion

Consider for a moment the classical homogeneous nucleation and crystal growth for a single polyethylene molecule of $x = 4300$ at $\Delta T = 50$ K. The dimensions for the lowest energy state are $L^* = 23.2$ nm and $W^* = 3.0$ nm. As discussed above, this is a stable *equilibrium* chain folded crystal. Equilibrium because a crystal of the same volume that is different in any dimension has a higher free energy, and it is impossible to have a larger crystal. It is chain folded because the crystal thickness L^* is much less than $L_{\text{max}} = 109$ nm. Bear in mind that folding is inferred only from the L dimension, the folds being implicitly crystallographic. What Muthukumar²¹ did was to use the chainlike nature of the polymer molecule to develop the entropic $\ln Z$ contribution to the free energy in eqs 7 and 8, a step that, among other things, stands in mathematically for the statement “it is impossible to have a larger crystal”. Specifically, the number of chains n and degree of polymerization x in the term $n \ln Z$ of eq 7 bound the size of the crystal that may form, and this limit leads to the minimum in ΔG that establishes equilibrium dimensions. Restricting the amount (volume V) of crystallizable material in the classical eq 1 leads to a comparable equilibrium state. Hence, the polymer theory in eqs 7 and 8 is not fundamentally different from classical theory (eq 1), provided the system size is prescribed in the latter. Polymer theory does give results that differ in detail from those from classical nucleation and growth: equilibrium length $lm^* = 39.8$ nm, equilibrium width $\mu^{*1/2}b = 2.2$ nm, and $\phi_{\text{am}} = 0.052$ of the chain is noncrystalline. Again one has an equilibrium chain folded crystal, the polymer model having a greater thickness (and correspondingly smaller width) and a measurable amorphous fraction that derive from the chainlike nature of the material expressed by $\ln Z$. Recall that the larger aspect ratio results from the entropic increase of the effective “ σ_e ” and that part of this entropy comes from fold or loop configurations. Gaussian statistics for the loops facilitates the description of disordered folds and provides an analytical expression for the overall surface entropy (see Appendix). One should not infer that the loops are Gaussian, as such features violate the need to maintain both chain connectivity and a realistic mass density on the fold surface.²⁷ For small systems in which the total number of stems $n\mu$ is less than 50–100, it is likely that the transverse crowding implicit with Gaussian loops can be relieved by occupying an area greater than W^2 . In any case, the consequence of disordered (Gaussian) loops is the nonzero amorphous fraction ϕ_{am} . Having disordered folds or loops described by other statistics would likewise have ϕ_{am} increasing with T_c as in Figure 6 (see the Appendix). If one insists on adjacent reentry folds with perfect (crystallographic) regularity,

then the classical nucleation and growth model is appropriate and φ_{am} is always zero.

The present analysis underscores the fact that a small system will form a small crystal with small equilibrium dimensions. As small thickness in a polymer crystal requires chain folding, equilibrium chain folded crystals are formed; this conclusion is independent of the nature of the folds, be they Gaussian loops, crystallographic folds, or features having intermediate disorder. Should the system size be increased, equilibrium dimensions will increase with the cube root of crystal volume $V^{1/3}$ at constant aspect ratio L^*/W^* (or, equivalently, $m^*/(n\mu^*)^{1/2}$). In contrast to the critical nucleus dimensions, equilibrium crystal dimensions are relatively independent of undercooling, being established by system size (V) and aspect ratio.

How relevant are these equilibrium concepts to polymer crystallization as it actually occurs? Crystallization of isolated or nearly isolated chains from very dilute solution provides the most promising scenario. Here primary nucleation must be by chain folding, and single chain crystals are small and most likely to possess the mobility necessary to achieve equilibrium. Bittiger and Husemann²⁸ studied fractions of cellulose tricarbanilate crystallized from very dilute solutions. For fractions with $x > 1500$ the solid appeared as cylinders with $L \approx 60$ nm and diameter $D \approx 20$ nm. While surface energies are not known, the shape is qualitatively that expected for a polymer with $\sigma_e > \sigma_s$, and particle volumes corresponded exactly to those for single chains in the crystalline state for the known molecular weights of the fractions. Similar investigations of unfractionated ultrahigh molecular weight polyethylene ($x_w \approx 2 \times 10^5$) quenched from dilute solution gave particles of different shapes composed of a few chains.²⁹ Many of the crystals appear to be rodlike, although the aspect ratio of ca. 3 is about half that expected from the surface energies of polyethylene (eq 4). In neither study was the chain orientation within the rodlike crystals confirmed by diffraction; the cylinder axis was assumed to be the chain axis. Geil et al.³⁰ have recently reported on rodlike single crystals of poly(tetrafluoroethylene), $L \approx 100$ nm and $D \approx 20$ nm, that have volumes consistent with a single molecule of $x_w \approx 5 \times 10^5$. Isolated chains are grown by "nanoemulsion" polymerization, although the relation between polymerization mechanism and the formation of a single chain crystal is not settled. Other experiments on single chain crystals of high molecular weight poly(ethylene oxide),^{29,31} fractionated³² and unfractionated³³ isotactic polystyrene, fractionated *trans*-1,4-polyisoprene (gutta percha),³⁴ and fractionated *cis*-1,4-polybutadiene³⁵ employed crystallization by heating and/or cooling molecules that had been separated in a previous step. In such experiments the solidification from the single chain "melt" results in a variety of crystal shapes, most being lamellar in nature ($W > L$), which shows that equilibrium is less likely when crystallizing from a dense state. It goes without saying that crystallization from the melt does not give equilibrium structures. The critical homogeneous nucleus is much more likely to resemble a fringed micelle than a folded chain crystal, and the equilibrium habit is an extended chain because the number of chains $n > n_{\text{ec}}$.

Additional manifestations of thermodynamic control of folded chain polymer crystals are less direct. Lauritzen and Hoffman³ posited that folded chain primary nuclei form in dilute solution with a thickness near L_c that is pinned by fold immobility; recall that the critical dimensions (eq 2) are established solely by thermodynamics and that a crystal of thickness L_c can be stabilized by transverse growth. LH further asserted that this primary nucleus is the substrate upon which a thinner folded

chain crystal grows by secondary nucleation (kinetic control) with $L \sim L_c/2$. Geil^{36,37} observed by electron microscopy protuberances at the center of solution grown crystals; these primary nuclei are some 2–4 times thicker than the lamellar crystals, an observation that supports the LH concept that folded primary nuclei are unable to thicken. Blundell and Keller³⁸ have shown that similar primary nuclei (seeds) in polyethylene are small polymer crystals that are unusually resistant to dissolution. Such structures are thought to be nanoscopic monomolecular crystals that thicken (move toward equilibrium dimensions) during the heating/dissolution step before subsequent "seeded" crystallization. As they are stable in the presence of solvent, they should have thickness $L > L_c$. So nuclei for solution crystallization, regardless of the method of their formation, conform to the LH notion of small, folded chain crystals with thickness approximating L_c .

While the primary focus of this work is equilibrium folded chain crystals, the entropic $\ln Z$ term in the polymer theory leads to the crystal thickness L^* becoming smaller at larger T_c (see Figure 5). A related effect is reversible surface melting that was mentioned earlier. The first unambiguous demonstration of this process was presented by Burmester and Geil.³⁹ Wide-angle diffraction peak widths showed the thickness of polyoxymethylene crystals to decrease reversibly by ca. 3 nm as the final melting temperature was approached. A more recent small-angle X-ray study of polyethylenes by Albrecht and Strobl reveals clearly that the amorphous layer thickens reversibly by about 5 nm (ca. 100%) in the range below T_m . While such surface melting is not for equilibrium crystals, it nevertheless confirms the importance of the surface entropy contribution that gives rise to the temperature-dependent amorphous fraction φ_{am} in Figure 6. It is possible that the Gaussian loops employed in the polymer model lead to φ_m being unrealistically large, but that does not negate the basic idea that fold surface disorder increases with temperature.

Simulations are likely to reveal equilibrium crystallization because computational limitations favor small systems that have sufficient mobility to achieve the lowest free energy. The seminal molecular dynamics simulations of Kavassalis and Sundararajan²⁰ were mentioned earlier. Folded chain crystals are evident with aspect ratio $L/W \approx 2$, but it is not known what the equilibrium shape should be with the energy parameters employed. Other aspects of that work confirm equilibrium features discussed above. When system size was reduced by 50% (x decreased from 500 to 250 united atom beads), the average crystal length L decreased from 4.3 to ~ 3 nm. When system size was increased 4-fold (n raised from 1 to 4), L increased from 3 to 5 nm. In both cases the crystal thickness $L \sim V^{1/3}$ as suggested for equilibrium by eq 3. In addition, increasing the crystallization temperature led to structures having thinner crystalline regions with more internal and surface disorder, again in accord with the behavior of equilibrium systems. In a subsequent paper⁴⁰ the same authors demonstrated that increasing the basal surface energy σ_e (by stiffening the intrachain torsional potential) increased thickness L in qualitative agreement with eq 3.

Muthukumar and co-workers have published simulations of polymer crystallization with up to 10 000 united atoms. The first paper by Liu and Muthukumar⁴¹ established that integral folding is favored (cilia lengths are small), an observation that harks back to the equilibrium approach of Peterson and Lindenmeyer.⁷ For chains with $x = 500$ beads, the linear dimension of the nucleus (the structure first formed) was found to be inversely proportional to undercooling ΔT , the expectation

for critical (eq 2) or stability (eq 5) dimensions. In another study with Welsh, isothermal crystallization of a single chain with $x = 2000$ beads clearly showed the formation of two nuclei that grow to form one folded chain crystal.⁴² A significant feature is that the crystal thickness L and width W each double during this process with a constant aspect ratio of 2.3. Subsequent work by Welsh and Muthukumar⁴³ documented the equilibrium nature of folded chain crystals formed by chains of $x = 200$ beads; the energy profile derived from relative populations has three local minima at increasing thickness L , the deepest minimum being for four folds per chain. Additionally, a multichain crystal thickened by 33% as the number of chains n increased 4-fold, which is over half of the 58% increase predicted by eq 3. In the most recent paper of that series Muthukumar²¹ obtained free energy profiles as described above for chains of different length. The lowest energy (equilibrium) thickness L^* increased by 10% when x was raised from 200 to 300, an increment that is near the 14% change estimated from eq 3.

While the case for small chain folded crystals with thermodynamically controlled shape is a reasonable one, it is certain that equilibrium dimensions cannot be maintained with continued growth. The difficulty is with the crystal thickness or fold period L ; an existing crystal must increase its fold period to maintain the equilibrium aspect ratio as stems are added ($L^* \sim W^* \sim V^{1/3}$). Without speculating on the mechanism for such a rearrangement (see for instance Figure 1 of ref 43), it is undoubtedly a highly cooperative one that is more feasible in a small crystal with a few short stems; large crystals are expected to thicken sluggishly or not at all. The implication is that L will grow somewhat from the critical L_c value and then become kinetically trapped, while the extreme view is that the thickness is maintained at L_c . One might suppose that another factor limiting L during crystal growth is the familiar role of secondary nucleation barriers. If, however, rearrangement of the fold length were facile, then layers of stems that add with a kinetically controlled thickness would soon evolve to the equilibrium L^* . In fact, the inability of thin, nonequilibrium crystals to thicken is essential for the kinetic approach to chain folding first advocated by Lauritzen and Hoffman.

Simulations provide insight on how crystal dimensions, particularly thickness L , are established. Larger undercooling and/or long chains favor the formation of one or more compact nuclei, each comprising only a fraction of a chain. These small ordered structures enlarge and coalesce, following a path of nucleation and growth like that in Figure 3b. Examples of this expected behavior can be found in studies with single chains of $x \geq 1000$ beads by Kavassalis and Sundararajan²⁰ and by Muthukumar and Welch.⁴² If undercooling ΔT and/or degree of polymerization x are small, the critical nucleus may comprise virtually the whole chain and be unstable. An example of fluctuations between a two-stem "nucleus" and the solution state for a chain of only 30 beads is presented by Sundararajan and Kavassalis,⁴⁰ and similar effects were described without illustration for a chain of 700 united atoms by Liu and Muthukumar.⁴¹

The unique interplay between chainlike matter and crystallization may be operative in what has been termed "global collapse" by Kavassalis and Sundararajan.²⁰ The entire amorphous chain rearranges from an open conformation to a compact one that subsequently converts to the stable crystalline state as a unit, translational order being established in all parts of the system more or less simultaneously. Liu and Muthukumar report the same process for a single 700-unit chain and for a collection of 13 chains of 154 beads.⁴¹ This mechanism clearly does not conform to nucleation and growth as delineated by the solid

arrow in Figure 3b; there is no small ordered nucleus that forms first, and the crystal dimensions L and W appear to be established by the size of the compact amorphous intermediate state. The aspect ratio of crystals formed by this route is about the same as those formed by nucleation and growth.

The concept that crystallization from dilute solution proceeds through a globally collapsed amorphous state has been advocated by Qian,⁴⁴ who argues that such collapse is inevitable because the polymer-solvent system is below the Flory θ temperature. Collapsed chains contain loops that are the precursors of folds in the crystalline state. The idea of "prefolded" amorphous chains (or sections of chains) is certainly supported by some of the simulations described above. Lindenmeyer was among the first to suggest that polymer crystals grow by accretion of prefolded chains.⁴⁵ Shortly thereafter, Allegra advanced a detailed "bundle theory" for crystallization of metastable, prefolded chains nearly 30 years ago.⁴⁶ Prefolded chains have also been proposed to account for the growth of certain lathlike polymer crystals in the direction of folding.⁴⁷ At a more general level, polymer crystallization has two special attributes not found in other systems: a predefined set of crystallizable units are correlated by covalent bonds, and a huge number of disordered states (approximately x^3 per chain) are possible. One or both of these features are likely responsible for simulated crystallization through global collapse. It is not known whether this global collapse mechanism operates in actual crystallization from dilute solution, as the capture of such a fleeting intermediate is an unmet challenge.

Conclusions

Homogeneous primary nucleation inevitably creates crystals with small dimensions that are dictated by (unstable) thermodynamic equilibrium conditions, not by kinetics. A flexible polymer chain in dilute solution must form a folded chain nucleus with thickness L_c that becomes stable on spontaneous growth in the thickness L and/or width W directions. There is little fundamental difference between classical nucleation and growth and that for polymers, although the latter allows for explicit evaluation of the effects of folds and cilia on the free energy that lead to an equilibrium amorphous fraction φ_{am} . Equilibrium growth of polymer crystals occurs at an aspect ratio L/W that is modestly greater than σ_e/σ_s from classical theory because the aforementioned entropy from loops and tails increases the effective basal specific surface energy of the crystal. The number of folds per chain drops during equilibrium growth. If sufficient polymer molecules are present to permit growth to $L = L_{max}$, the extended chain state becomes the equilibrium crystal habit. Hence, for small systems the equilibrium state is the chain folded crystal, while for large systems the equilibrium state is the familiar extended chain crystal. The entropic contribution of cilia and disordered folds results in an equilibrium noncrystalline fraction that increases reversibly with crystallization temperature.

A unique feature of polymer crystal growth is that an increase of equilibrium thickness L requires all previously crystallized stems to adopt new fold conformations, a process that certainly becomes sluggish as the size of the crystal increases in size. It is obvious that a similar growth restriction is not present for low molecular weight substances. Thus, conformity to equilibrium growth in polymers is expected primarily in small systems such as very dilute solutions or simulations of isolated or nearly isolated chains. Muthukumar has asserted that simulations support the notion of equilibrium chain folded polymer crystals.²¹ That conclusion is certainly correct for the small systems

in question, but it should not be extrapolated to large lamellar features such as those observed by Keller² (a $1\ \mu\text{m}^2$ lamella contains 5×10^6 stems of 120 CH_2 groups each, or about 6×10^8 “beads”), where secondary nucleation accounts for the temperature dependencies of both initial thickness and growth rate. An additional special feature may be seen during crystallization of one or a few chainlike molecules that define a small system with a large number of noncrystalline states. Here it is possible for crystalline order to develop simultaneously throughout the entire system via global collapse as opposed to nucleation and growth. The relevance of this novel mechanism beyond simulations has yet to be established.

Acknowledgment. The author is indebted to H. Marand for preliminary discussions of the issues developed in this paper.

Appendix. Free Energy Expressions

Equation 8 differs from eq 4.2 of ref 21 in that a factor of $n^{-1/2}$ is included in the second σ_s term and the basal surface energy σ_e term is present. The factor of $n^{-1/2}$ properly scales the contribution of a single chain to the lateral free energy of the crystal; omitting it has the effect of increasing the effective “ σ_s ” for large n . The third term for conventional basal surface energy σ_e is included to permit a direct link to classical nucleation theory, eq 1. Furthermore, the σ_e term in eq 8 enables one to observe unambiguously the effect of the entropic $\ln Z$ term on the free energy surface (compare Figure 3b to Figure 3a).

The probability factor Z for a single chain associated with a folded chain crystal is given by Muthukumar²¹ as

$$Z = 4 \left(\frac{1}{\nu a_0} \right)^{\mu-1} (x_k - \mu m_k) \left[\left(\frac{y^2}{2} + \frac{1}{4} \right) \text{erfc}(y) - \frac{y e^{-y^2}}{2\pi^{1/2}} \right] \quad (9)$$

where

$$y = \frac{(\mu - 1)a_0}{2(x_k - \mu m_k)^{1/2}}$$

Note that $x_k - \mu m_k$ is the number of noncrystalline units that comprise the $\mu - 1$ loops and two tails. The loops obey Gaussian statistics in the half space above the crystal surface, so the repeat unit in this expression is a Kuhn segment of length $l_k > l$ and the number of Kuhn segments (not monomers) per chain is $x_k < x$. Cilia or tails are assumed to be short enough so their conformational entropy can be ignored. The parameter ν is a dimensionless volume on the order of l_k^3 , and a_0 is a dimensionless measure of the maximum end-to-end separation of a loop on the fold surface. Evaluation of Z here employs $\nu = \pi/(3\sqrt{6})$ and $a_0 = 8$, the values used by Muthukumar. The factors m and l in the first two terms on the right side of eq 8 are for monomers (e.g., C_2H_4 groups), not Kuhn segments; hence, there appears to be an inconsistency between these terms and $\ln Z$. But this is not the case, since the product ml (monomers) is equal to the product $m_k l_k$ (Kuhn segments), so eq 8 written in terms of “mixed” parameters for monomers and Kuhn segments is correct.

Larpini et al.⁴⁸ recently published a simulation and an analytical model that are basically the same as those in Muthukumar.²¹ Like Muthukumar, they omit the factor of $n^{-1/2}$ in the σ_s term and omit the σ_e term of eq 8. Those authors propose a simpler, more approximate form of Z that omits the conformational entropy of loops (assumed to be rather tight folds). The divergence of $\ln Z$ as $\mu m_k \rightarrow x_k$ gives rise to the

free energy trough and establishes equilibrium dimensions. A surprising result is that the equilibrium amorphous fraction $\varphi_{\text{am}} = 0.23$ is very large, even though the loops are assumed to be short and non-Gaussian. The entropic $\ln Z$ term is the only source of basal free energy (effective “ σ_e ”) that establishes critical m_c and equilibrium m^* in both Larpini and Muthukumar.

Chen et al.¹⁷ similarly employed a term based on loop entropy for the basal surface energy of a single chain crystal, together with a conventional lateral σ_s term. They assume that the fraction of material in the loops is very small and simplify the expression to give equilibrium dimensions equivalent to the classical result eq 3 (no amorphous fraction φ_{am}).

References and Notes

- (1) Storks, K. H. *J. Am. Chem. Soc.* **1938**, *60*, 1753.
- (2) Keller, A. *Philos. Mag.* **1957**, *2*, 1171.
- (3) Lauritzen, J. I.; Hoffman, J. D. *J. Res. Natl. Bur. Stand. A* **1960**, *64*, 73.
- (4) Hoffman, J. D.; Lauritzen, J. I. *J. Res. Natl. Bur. Stand. A* **1961**, *65*, 297.
- (5) Armistead, K.; Goldbeck-Wood, G. *Adv. Polym. Sci.* **1992**, *100*, 221.
- (6) Peterlin, A.; Fischer, E. W.; Reinhold, C. *J. Chem. Phys.* **1962**, *37*, 1403.
- (7) Peterson, J. M.; Lindenmeyer, P. H. *Makromol. Chem.* **1968**, *118*, 343.
- (8) Flory, P. J. *J. Chem. Phys.* **1949**, *17*, 223.
- (9) Mandelkern, L.; Fatou, J. G.; Howard, C. *J. Phys. Chem.* **1964**, *68*, 3386; *J. Phys. Chem.* **1965**, *69*, 956.
- (10) Zachmann, H. G. *Kolloid Z. Z. Polym.* **1967**, *216–217*, 180.
- (11) Wunderlich, B. *Macromolecular Physics*; Academic Press: New York, 1976; Vol. 2, pp 16–35, Chapter 5.
- (12) Zachmann, H. G.; Peterlin, A. *J. Macromol. Sci., Phys.* **1969**, *B3*, 495.
- (13) Wunderlich, B. *Macromolecular Physics*; Academic Press: New York, 1980; Vol. 3, pp 234–236.
- (14) Schultz, J. M.; Robinson, W. H.; Pound, G. M. *J. Polym. Sci., Part A-2* **1967**, *5*, 511.
- (15) Albrecht, T.; Strobl, G. *Macromolecules* **1995**, *28*, 5827.
- (16) Ishinabe, T. *J. Chem. Phys.* **1978**, *15*, 1808.
- (17) Chen, E.; Bu, H.; Hu, X. *Macromol. Theory Simul.* **1994**, *3*, 409.
- (18) Flory, P. J.; Vrij, A. *J. Am. Chem. Soc.* **1963**, *85*, 3548.
- (19) Hoffman, J. D.; Miller, R. L.; Marand, H.; Roitman, D. B. *Macromolecules* **1992**, *25*, 2221.
- (20) Kavassalis, T. A.; Sundararajan, P. R. *Macromolecules* **1993**, *26*, 4144.
- (21) Muthukumar, M. *Philos. Trans. R. Soc. London A* **2003**, *361*, 539.
- (22) Hoffman, J. D.; Miller, R. L. *Polymer* **1997**, *38*, 3151.
- (23) Wulff, G. *Z. Kristallogr.* **1901**, *34*, 449.
- (24) Wunderlich, B. *Macromolecular Physics*; Academic Press: New York, 1973; Vol. 1, p 182.
- (25) Hu, W.; Frenkel, D.; Mathot, V. B. F. *Macromolecules* **2003**, *36*, 8178.
- (26) Gibbs, J. W. *Collected Works*; Yale University Press: New Haven, CT, 1948; Vol. 1, p 55.
- (27) Flory, P. J.; Yoon, D. Y.; Dill, K. A. *Macromolecules* **1984**, *17*, 862.
- (28) Bittiger, H.; Husemann, E. *Makromol. Chem.* **1966**, *96*, 92.
- (29) Bu, H.; Pang, Y.; Song, D.; Yu, T. Voll, T. M.; Czornyj, G.; Wunderlich, B. *J. Polym. Sci., Part B: Polym. Phys.* **1991**, *29*, 139.
- (30) Geil, P. H.; Yang, J.; Williams, R. A.; Petersen, K. L.; Long, T.-C.; Xu, P. *Adv. Polym. Sci.* **2005**, *180*, 89.
- (31) Cao, J.; Gu, F.; Liu, Y.; Bi, S.; Bu, H.; Zhang, Z. *Macromol. Symp.* **1997**, *124*, 89.
- (32) Bu, H.; Chen, E.; Xu, S.; Guo, K.; Wunderlich, B. *J. Polym. Sci., Part B: Polym. Phys.* **1994**, *32*, 1351.
- (33) Bu, H.; Gu, F.; Chen, M.; Rao, L.; Cao, J. *J. Macromol. Sci., Phys.* **2000**, *B39*, 93.
- (34) Su, F.; Yan, D.; Liu, L.; Luo, J. Shou, E.; Qian, R. *Polymer* **1998**, *22*, 5379.
- (35) Liu, L.; Li, H.; Jiang, Z.; Zhou, E.; Qian, R. *Makromol. Chem., Rapid Commun.* **1993**, *14*, 747.
- (36) Geil, P. H. *Polymer* **1963**, *4*, 404.
- (37) Geil, P. H. *Polymer* **2000**, *41*, 8983.
- (38) Blundell, D. J.; Keller, A. *J. Macromol. Sci., Phys.* **1968**, *B2*, 301.
- (39) Burmester, A. F.; Geil, P. H. In *Advances in Polymer Science and Engineering*; Pae, R. D., Morrow, D. R., Chen, Y., Eds.; Plenum Press: New York, 1972; pp 43–100.
- (40) Sundararajan, P. R.; Kavassalis, T. A. *J. Chem. Soc., Faraday Trans.* **1995**, *91*, 2541.
- (41) Liu, C.; Muthukumar, M. *J. Chem. Phys.* **1998**, *109*, 2536.
- (42) Muthukumar, M.; Welch, P. *Polymer* **2000**, *41*, 8833.
- (43) Welsh, P.; Muthukumar, M. *Phys. Rev. Lett.* **2001**, *87*, 218302.
- (44) Qian, R. *J. Macromol. Sci., Phys.* **2001**, *B40*, 1131.

- (45) Lindenmeyer, P. H. *Polym. Eng. Sci.* **1974**, *14*, 456.
- (46) Allegra, G. *J. Chem. Phys.* **1977**, *66*, 5453. Allegra, G.; Meille, V. *Phys. Chem. Chem. Phys.* **1999**, *1*, 5179.
- (47) Marchessault, R. H.; Kawada, J. *Macromolecules* **2004**, *37*, 7418.
- (48) Larini, L.; Barbieri, A.; Pevosto, D.; Rolla, P. A.; Leporini, D. *J. Phys.: Condens. Matter* **2005**, *17*, L199.

MA0520343